Nanoscale

Nitrogen and Sulfur Co-doped Carbon Dots with Strong Blue Luminescence

Journal:	*Nanoscale*
Manuscript ID:	NR-ART-07-2014-004267.R1
Article Type:	Paper
Date Submitted by the Author:	11-Sep-2014
Complete List of Authors:	Ding, Hui; Fudan University, Wei, Ji-Shi; Fudan University, Xiong, Huan-Ming; Fudan University, Chemistry

Journal Name

RSCPublishing

ARTICLE

Nitrogen and Sulfur Co-doped Carbon Dots with Strong Blue Luminescence

Cite this: DOI: 10.1039/x0xx00000x

Hui Ding, Ji-Shi Wei, Huan-Ming Xiong*

Received 00th January 2012,
Accepted 00th January 2012

DOI: 10.1039/x0xx00000x

www.rsc.org/

Sulfur-doped carbon dots (S-CDs) with quantum yield (QY) of 5.5% and nitrogen, sulfur co-doped carbon dots (N,S-CDs) with QY of 54.4% were synthesized respectively via the same hydrothermal route using α-lipoic acid as the carbon source. The obtained S-CDs and N,S-CDs had similar sizes but different optical features. The QY of N,S-CDs was gradually enhanced when extending reaction time to increase the nitrogen content. After careful characterizations on these CDs, the doped nitrogen element was believed in form of C=N and C-N bonds which enhanced the fluorescent efficiency significantly. Meanwhile, the co-doped sulfur element was found to be synergistic for nitrogen doping in N,S-CDs. The optimal N,S-CDs were successfully employed as good multicolor cell imaging probes due to their fine dispersion in water, excitation-dependent emission, excellent fluorescent stability and low toxicity. Besides, such N,S-CDs showed a wide detection range and excellent accuracy as fluorescent sensors for Fe^{3+} ions.

1. Introduction

Carbon dots (CDs), as a new type of photoluminescent (PL) nanomaterials, have received much attention due to their low cost, outstanding biocompatibility and unique physical properties in the past decade.[1, 2] Scientists have produced various CDs by both top-down methods and bottom-up strategies,[3-7] and applied them in many fields.[8-12] For example, CDs synthesized via electrochemical method were used to prepare highly efficient catalysis for photodegradation of methyl blue;[5] Strongly luminescent CDs produced by hydrothermal method were applied for multicolor patterning, Fe^{3+} detection and cell imaging;[10] Nitrogen-rich CDs prepared by emulsion-templated carbonization were dispersed into polymer matrix to fabricate luminescent films for lighting systems.[13] Among these unique properties of CDs, PL is most amazing because CDs' fluorescence depends on the excitation conditions and the raw materials heavily, which is distinguished from other semiconductor nanoparticles.[14, 15] The raw materials for CDs vary from organic chemicals at lab to those natural biomaterials like soy milk,[16] orange juice[17] and hair fiber.[18] CDs with the same sizes but made from different raw materials always exhibit quite different PL phenomena.[19] Therefore, controlling the compositions and structures of CDs is a key to understand their complicated luminescent mechanisms.

Doping CDs with other non-metallic elements is able to adjust their compositions and structures. For instance, Zhang et al. prepared N-doped CDs with tunable luminescence by adjusting N contents;[20] Qian et al. improved the QY of CDs by incorporating nitrogen and speculated that the fluorescence enhancement originated from the polyaromatic structures induced by the doped nitrogen.[21] Sun et al. prepared a highly luminescent N-doped carbon dots with their QY up to 94% and ascribed the high yield of radiative recombination between the trapped electrons and holes to a newborn surface state induced by the nitrogen in CDs;[22] By far, plenty of work focused on the nitrogen doped CDs, but the CDs containing sulfur dopant[23] and co-dopants[24] were rarely reported. In addition, although nitrogen doping were usually found to enhance CDs fluorescence,[21] the corresponding mechanisms remain unclear. And thus, it is a challenge to study the synergistic effects by two dopants, and meanwhile, search for the origin of the luminescence enhancement through controlling the CD compositions.

In the present work, we compared the sulfur-doped CDs and the nitrogen, sulfur co-doped CDs with similar particle sizes. Both of them were synthesized via one-step hydrothermal route using α-lipoic acid as the carbon source, but their fluorescent properties were quite different. After careful characterizations, C=O groups on the CD surface were considered as the main emission centers for blue luminescence, while C=N and C-N bonds in form of polyaromatic structures were proved to be the key factors of promoting fluorescence of N,S-CDs. The sulfur atoms existed in N,S-CDs were confirmed to be synergistic for doping nitrogen in CDs. The obtained N,S-CDs exhibited strong blue emission with QY of 54.4%, low cytotoxicity, high sensitivity towards Fe^{3+} ions and multicolor imaging function for the living cells.

2. Experimental section

2.1 Synthesis of S-CDs and N,S-CDs.

For Sulfur-doped carbon dots (S-CDs), 0.1 g of NaOH was dissolved into 50 ml of DI-water to get a basic solution. Then 0.5 g of α-lipoic acid was added and stirred to obtain pale yellow solution. After that, the solution was transferred into a poly(paraphenol)-lined stainless steel autoclave and heated at 250℃ for 1, 3, 7, 11, 15 and 19 hours. After cooling down to room temperature, the obtained solution was purified via dialysis through an analysis membrane (Spectrum, MW cutoff 3500). For Nitrogen and sulfur co-doped carbon dots (N,S-CDs), 0.5 g of α-lipoic acid，0.1 g of sodium hydroxide and 0.3 g of ethylenediamine were added into 50 ml of H_2O and then stirred to obtain pale yellow solution. The subsequent treatments were the same with those for S-CDs. Finally, two CDs aqueous solutions were freeze-dried for characterizations.

2.2 Synthesis of N-CDs.

0.5 g of 3-cyclopentylpropionic acid and 0.3 g of ethylenediamine were dissolved in 50 ml of pure water. Then, 0.1 g of sodium hydroxide was also added. The obtained colorless transparent solution was performed the same treatments with those for S-CDs.

2.3 Reduction of N,S-CDs.

Excess $NaBH_4$ was added into N,S-CDs aqueous solution and the mixture was stirred at room temperature for 4 h. After the reaction, the product was transferred into a dialysis bag and dialyzed for 2 days.

2.4 Fluorescent sensors for Fe^{3+} detection.

The freeze-dried N,S-CDs powder was dissolved in a PBS solution (pH = 7.4) with a concentration of 0.1 mg/mL. And then, aqueous solutions containing thirteen kinds of metal ions, Na^+, K^+, Sn^{4+}, Cu^{2+}, Zn^{2+}, Fe^{3+}, Ba^{2+}, Mg^{2+}, Co^{2+}, Fe^{2+}, Ca^{2+}, Al^{3+} and Pb^{2+}, were prepared respectively with their concentrations of 1 mM. To evaluate the selectivity of N,S-CDs, 100 μL of the above metal ions solution was mixed with 900 μL of the N,S-CDs solution, and then the PL spectra were measured for recording the fluorescence intensity. To evaluate the detection range of Fe^{3+}, 100 μL of the solutions containing different concentrations of Fe^{3+} were mixed with 900 μL of the N,S-CDs solution respectively. The control sample was prepared by mixing 100 μL of pure water with 900 μL of the N,S-CDs solution. All the samples were excited at 390 nm, and the intensities of fluorescence emission at 472 nm for each sample were recorded for comparison.

2.5 Cytotoxicity assay.

Hela cells were seeded in a 96-well cell culture plate in Dulbecco's modified Eagle medium (DMEM) at a density of 5×10^4 cells per mL with 10% fetal bovine serum (FBS) at 37℃ and with 5% CO_2 for 24 h. Afterwards, the culture medium was replaced with 200 μL of DMEM containing the carbon dots at different doses and cultured for another 48 h. And then, 20 μL of 5 mg/mL MTT (3-(4,5-dimethylthiazol-2yl)- 2,5-diphenyltet razolium bromide) solution was added to every cell well. The cells were further incubated for 4 h, followed by removing the culture medium with MTT, and then 150 μL of DMSO was added. The resulting mixture was shaken for 15 min at room temperature. The absorbance of MTT at 492 nm was measured on an automatic ELISA analyzer (SPR-960). The control data was obtained in absence of CDs. Each experiment was conducted 5 times and the average data was present.

2.6 Multicolor cell imaging.

Cellular fluorescent images were recorded by a Leica Tcs sp5 Laser Scanning Confocal Microscope. HeLa cells were seeded in 6-well culture plates at a density of 10^5 per well in DMEM containing 10% fetal bovine serum (FBS) at 37 ℃ in a 5% CO_2 incubator for 24 h. After removing DMEM, the mixture of N,S-CDs (100 μg/mL) in the DMEM medium was added into each well for 2 h incubation. Finally, the cells were washed twice by phosphate buffer solution (PBS) to remove extracellular CDs and were then fixed with 4% paraformaldehyde.

2.7 Quantum yield (QY) measurements.

Quantum yield (QY) was measured by an integrating sphere attached to a Horiba Jobin Yvon fluoromax-4 spectrofluorometer. Firstly, the aqueous solution of N,S-CDs was diluted to keep absorption intensity under 0.1 at the best excitation wavelength of 390 nm. Subsequently, the aqueous solution was added into the 10 mm fluorescence cuvette, placed in the integrating sphere and excited by monochromatic light of 390 nm. We recorded the fluorescence spectrum of our sample in the ranges of 380-400 nm and 405-750 nm, respectively. Meanwhile, we also recorded the same fluorescence spectrum of pure water under the same conditions. Finally, we used the fluorescent software to calculate the QY of our samples. Each experiment was conducted three times in parallel and the average value of QY was worked out. Besides, QY of N-CDs was also tested with the same conditions because of their similar PL spectra. In addition, we recorded the fluorescence spectrum of S-CDs in the ranges of 360-380 nm and 385-720 nm respectively because the best excitation wavelength for S-CDs was 370 nm. The other measurement conditions were the same with those for N,S-CDs.

3. Results and discussion

3.1 Characterization of S-CDs and N,S-CDs.

S-CDs were obtained by hydrothermal treatment on the basic aqueous solution of α-lipoic acid in poly(para phenol)-lined stainless steel autoclaves under 250℃ for different times and then purified by dialysis against water. In the case of N,S-CDs, ethylenediamine was added into the same reaction systems together with α-lipoic acid, as illustrated in Scheme S1. All the samples selected for characterization were prepared at 250℃ for 19 hours, except those pointed out especially.

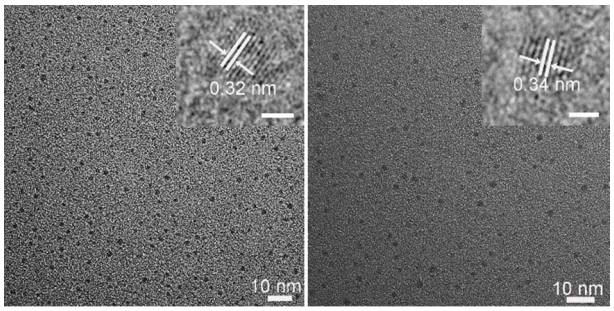

Fig. 1 TEM and HRTEM (inset) images of the as-prepared S-CDs (left) and N,S-CDs (right). The scale bar represents 2 nm in the inset images.

The transmission electron microscopy (TEM) images (Figure 1) show that the S-CDs and N,S-CDs are uniform and well dispersed with an average diameter of 2.5 and 2.7 nm, respectively (see Figure S1). The high-resolution TEM (HRTEM) image of S-CDs in Figure 1 shows the well-resolved lattice fringes with an average interplanar spacing of 0.32 nm, which is very close to the (002) diffraction facets of graphite.[24] Meanwhile, a similar result of 0.34 nm is found in N,S-CDs, indicating that both S-CDs and N,S-CDs have finished graphitization during reactions.[25] X-ray diffraction measurements show both samples have the same diffraction peak at around 23.1°, corresponding to an interlayer spacing of 0.38 nm. This value is a little larger than the result of HRTEM, owing to the existence of organic functional groups on CD surfaces (Figure S2).[2, 26]

The Raman spectra of the two CDs (Figure S3) show two peaks centered at 1351 and 1576 cm^{-1}, representing D and G bands of carbon material respectively.[27, 28] The intensity ratios I_D/I_G referring to the ratio between the disordered structure and the graphitic structure are 0.93 and 0.86 respectively for S-CDs and N,S-CDs, indicating S-CDs are more disordered and amorphous than N,S-CDs.[2, 29] The higher graphitic extent of N,S-CDs may result from the polyaromatic structures induced by the incorporated nitrogen atoms and the protonation of nitrogen atoms on CD surfaces.[21, 30] The Raman results suggest that both CDs consist of graphitic sp2 carbon atoms in the crystalline cores and sp3 carbon defects on the surfaces or in the cores.[27, 31]

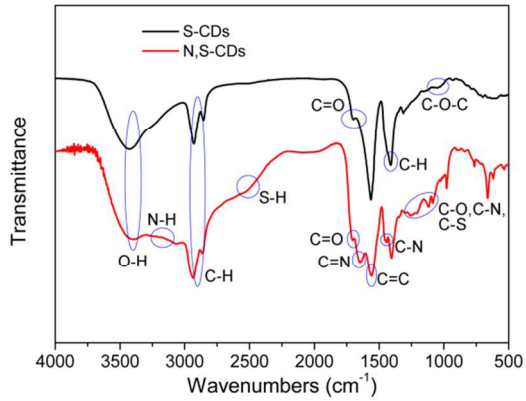

Fig. 2 FT-IR spectra for S-CDs and N,S-CDs.

The Fourier transform infrared (FT-IR) spectra of S-CDs and N,S-CDs (Figure 2) show the absorption bands at around 3420, 1562 and 2928 cm^{-1}, corresponding to the stretching vibrations of O-H/N-H, C=C and C-H respectively.[18, 29, 32] Both samples have similar IR bands within the range of 1000-1400 cm^{-1}, which are attributed to the stretching vibrations of C-O, C-S and C-H respectively.[24, 33] However, the C=O stretching vibration band at 1705 cm^{-1} in S-CDs shifts to 1670 cm^{-1} in the N,S-CDs, and a new band at 1122 cm^{-1} arises for the asymmetric stretching vibrations of C-NH-C, which confirms that ethylenediamine molecules are graphed onto the N,S-CD surfaces through amide bonds.[10, 33] Moreover, another two bands at 1640 and 1443 cm^{-1}, representing the typical stretching modes of C=N and C-N respectively in heterocycles, are only observed in N,S-CDs,[34, 35] suggesting that nitrogen atoms not only exist on the particle surface in form of amide bonds but also exist in the cores as polyaromatic structures.

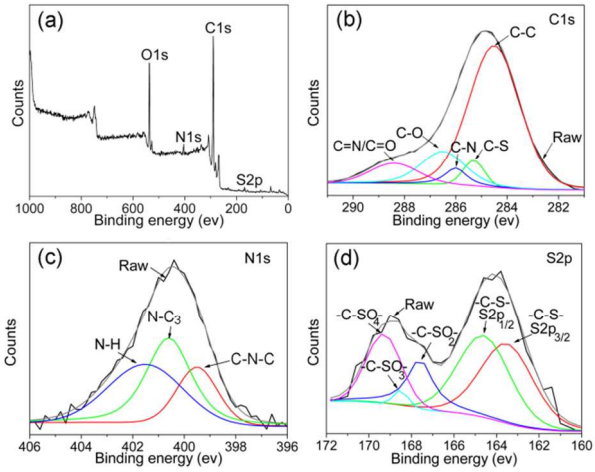

Fig. 3 (a) XPS spectra of the obtained N,S-CDs. (b-d) High-resolution XPS spectra of the C1s, N1s and S2p of the N,S-CDs, respectively.

The X-ray photoelectron spectra (XPS) are employed to investigate the surface states of S-CDs (Figure S4) and N,S-CDs (Figure 3). The wide spectrum of N,S-CDs (Figure 3a) shows four typical peaks of C1s (285 eV), N1s (400 eV), O1s (531 eV) and S2p (164 eV).[18, 24] The high-resolved C1s XPS spectrum (Figure 3b) can be deconvoluted to be five peaks at 284.5, 285.3, 286.0, 286.5 and 288.2 eV, which represent C1s states in C-C/C=C, C-S, C-N, C-O and C=O/C=N bonds respectively.[11, 18] The N1s spectrum (Figure 3c) displays three peaks at 399.5, 400.6 and 401.6 eV, which can be ascribed to pyridinic C-N-C, pyrrolic C_2-N-H and graphitic N-C_3,[21] respectively. The S2p spectrum (Figure 3d) confirms two main bands at 164.0 and 167.6 eV, which confirms sulfur in two groups of -C-S- and -C-SO_X- respectively. The former can be resolved into two peaks at 163.5 and 164.6 eV, which are assigned to the $2p_{3/2}$ and $2p_{1/2}$ of the -C-S- covalent bond respectively.[18] The latter can be deconvoluted into three peaks at 167.6, 168.5 and 169.3 eV, owing to -C-SO_x- (x = 2, 3, 4) species respectively.[36] The S2p spectrum of N,S-CDs is similar with that of S-CDs (Figure S4d), while the N1s spectrum of

N,S-CDs proves the newborn polyaromatic structures containing C-N and C=N, in accord with the FTIR analyses.

3.2 Blue luminescence of N,S-CDs.

The UV-visible absorption and fluorescence spectra of the S-CDs and N,S-CDs are compared in Figure 4. In Figure 4b, both samples exhibit similar absorption onset at 320 nm due to the trapping of excited-state energy by the surface states,[24, 37] but only N,S-CDs have a clear absorption peak at 270 nm, which may be ascribed to π-π* transition of C=N bonds.[8, 31, 38] In Figure 4 c and d, both samples exhibit the typical CDs fluorescence which depends on the excitation wavelength.[25] However, N,S-CDs show much stronger blue emission than S-CDs (Figure 4a), and its QY is up to 54.4%, much higher than that of S-CDs (5.5%). Such strong fluorescence is ascribed to the nitrogen doping undoubtedly.

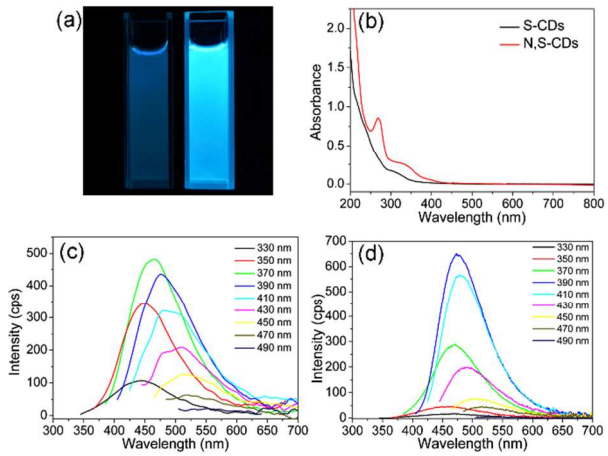

Fig. 4 (a) A photo of the obtained S-CDs (left) and N,S-CDs (right) under UV light (365 nm). (b) UV-visible absorption spectra of the S-CDs and N,S-CDs. (c, d) Fluorescence spectra of the S-CDs and N,S-CDs under different excitation conditions.

Although the fluorescence mechanisms for CDs are controversial at present, many researchers agree that quantum effects,[2, 39] surface states[24, 31] and carbogenic cores[10, 40] are the main factors that determine the emission features of CDs. In the present research, since S-CDs and N,S-CDs have similar particle sizes, the quantum effects can be excluded out of comparison. It is known that the composition of the CDs greatly influence the surface states and carbogenic cores of CDs,[24, 41, 42] so firstly we study CD performances by changing their compositions. For this purpose, both S-CDs and N,S-CDs are collected at different reaction time and measured by spectroscopic techniques. In Figure S5 and S6, the UV-Vis absorption and fluorescence spectra of the S-CDs synthesized at different time show almost no changes, indicating that the reaction time does not affect the optical properties of S-CDs significantly. On the contrary, the absorption spectra of N,S-CDs (Figure S7) show a feature peak at 270 nm increases gradually along with the reaction time, which means more and more C=N bonds are produced in this process.[25, 38] In the meantime, the blue emission at about 472 nm becomes stronger and stronger (Figure S8), and the main emission peak for N,S-CDs redshifts from 422 nm to 472 nm (Figure S9). According to the element analyses (Table S1) and XPS results (Table S2), extending reaction time can improve nitrogen doping extent, and produce more C-N, and C=N/C=O bonds. Hence, these newborn bonds are responsible for the strong blue emission definitely. As a result, the QY of N,S-CDs increases along with the nitrogen content (Figure S10 and S11), while the QY of S-CDs shows almost no changes when extending reaction time.

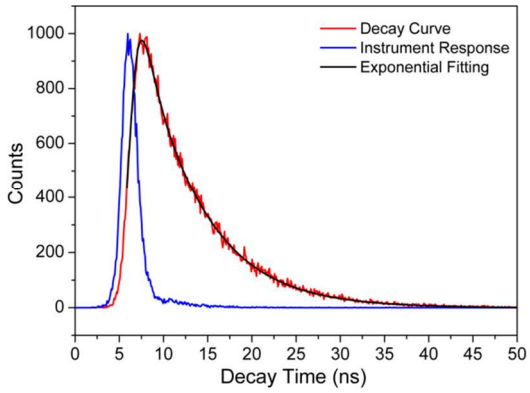

Fig. 5 Fluorescence lifetime of N,S-CDs measured by monitoring the emission at 472 nm when excited at 390 nm.

To further investigate the origin of CDs fluorescence, the fluorescence lifetime of both S-CDs and N,S-CDs are measured and compared in Figure 5, Figure S12 and Table S3, respectively. The fluorescence decay curves of all CDs samples can be fitted by a double-exponential formula,[29] involving the lifetime τ1 and τ2. For S-CDs, τ1 is about 1.5 ns while τ2 is about 3.8 ns, and their proportions are 43% and 57% respectively. For N,S-CDs, τ1 is about 2 ns while τ2 is about 6 ns, independent on the reaction time. However, the lifetime proportion of N,S-CDs changes continuously when extending the reaction time. On one hand, the average lifetime for N,S-CDs is longer than that of S-CDs, and increases gradually with extending reaction time, which means nitrogen doping in CDs produces more luminescent centers.[43] On the other, the τ2 proportion increases from 60.6% to 91.5% as the reaction time prolongs from 1 h to 19 h, indicating that τ2 is directly related with the N content and dominates the fluorescence properties of N,S-CDs. To further verify this point, we compare the transient fluorescence spectra of the τ2 at 6.54 ns collected by a fluorescence lifetime spectrometer (QM40) and the steady-state fluorescence spectra by a Horiba JobinYvon fluormax-4 spectrofluorometer in Figure S13. Both PL emission curves overlay with each other, so that C=N and C-N bonds are confirmed to be the origins for the enhanced QY of N,S-CDs.

It is known that sodium borohydride ($NaBH_4$) can selectively reduce some functional groups like C=N and C=O on CD surfaces.[31, 44] In Figure 6a, absorption spectra displays a clearly decrease at 320 nm after $NaBH_4$ treatment, indicating C=O functional groups are mostly reduced. But another absorption peak at 270 nm shows almost no change after $NaBH_4$ treatment, suggesting that C=N bonds mainly exist in

carbon cores.[21, 33] And the FT-IR spectra of the reduced N,S-CDs (Figure 6b) still have clear absorption at 1640 (C=N) and 1443 (C-N) cm^{-1} respectively, in accord with the UV-Vis absorption spectra. Figure 6c and 6d show that after C=O reduction, the maximum emission wavelength blue shifts from 470 nm to 410 nm,[45] while the QY of the reduced N,S-CDs is still as high as 45.9% when excited by 390 nm light, hence the high fluorescence efficiency of N,S-CDs is mainly ascribed to the C=N and C-N bonds existed in CD cores. According to the above analyses, we conclude that both C=O groups on the surfaces and the C=N/C-N bonds in CD cores are responsible for the blue emission of N,S-CDs, but the latter dominates when more and more nitrogen atoms are doped into CDs.

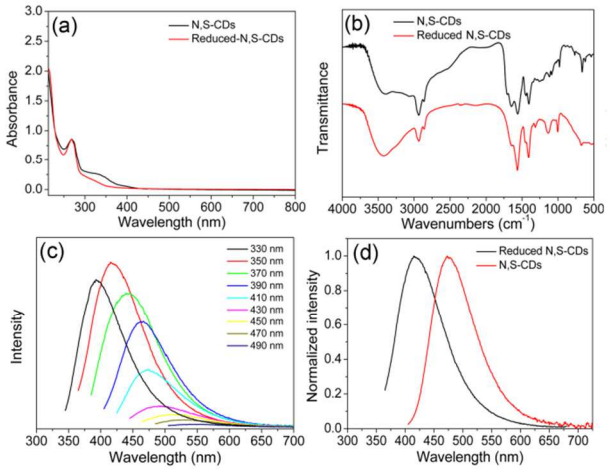

Fig. 6 (a) Absorption spectra of the N,S-CDs and the reduced N,S-CDs. (b) FT-IR spectra of the N,S-CDs (upper) and the reduced N,S-CDs (lower). (c) Fluorescence spectra of the reduced N,S-CDs. (d) The maximum emission peaks of the N,S-CDs and the reduced N,S-CDs.

3.3 Synergistic role of sulfur atoms.

In order to disclose the sulfur functions, nitrogen-doped carbon dots (N-CDs) were specially synthesized using 3-cyclopentylpropionic acid and ethylenediamine as starting materials and a similar route as shown in Scheme S2. Such N-CDs are monodispersed in water and have an average size of 2.6 nm (Figure S14), which is very close to that of N,S-CDs, suggesting the quantum effects can be ignored in comparisons.[31, 39] In the UV-Vis absorption spectra of such N-CDs (Figure S16), N-CDs also exhibit two absorption bands at 270 and 320 nm, owing to C=N and C=O bonds respectively.[46] But N-CDs exhibit much lower absorption at 270 nm than N,S-CDs, indicating the lower content of C=N bonds in N-CDs. The PL spectra (Figure S15) show the maximum emission at 472 nm is obtained by excitation at 390 nm, implying the fluorescent centers of N-CDs are similar with those of N,S-CDs.[24, 47] Besides, the absorption spectra and PL spectra for the N-CDs synthesized by extending reaction time are recorded in Figure S17 and Figure S18, respectively. Both the characteristic UV-Vis absorption band at 270 nm and the characteristic PL emission at 472 nm increase gradually when prolonging the reaction time, confirming that more and more nitrogen element are doped into CDs. The QY evolution curves of S-CDs, N-CDs and N,S-CDs are compared in Figure S10. Although the three curves display the similar increasing trend until the highest QY, the optimal QY of N-CDs is 20.1%, which is lower than the 54.4% of N,S-CDs but higher than the 5.5% of S-CDs. Therefore, we confirm that the co-doped sulfur atoms in N,S-CDs can help enhance the effect of nitrogen doping as a synergistic role.[24] It has been reported that the sulfur and nitrogen co-doped carbon materials exhibit higher catalytic activity towards the oxygen reduction reaction in comparison with the nitrogen-doped carbon materials through a cooperative effect.[48-50] In addition, DFT calculations revealed that the synergistic enhancement on the CDs performances was from the redistribution of spin and charge densities after the dual doping of S and N atoms.[48] In our work, sulfur atoms doping gives CDs more opportunities to form C=N bonds, as confirmed by the enhanced absorption at 270 nm. And thus, we think that redistribution of spin and charge densities in the CDs is the basis of synergetic effects.

3.4 Fe^{3+} detection and multicolor cell imaging.

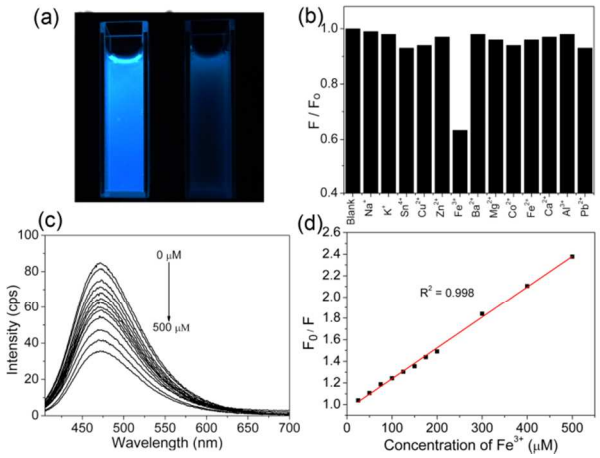

Fig. 7 (a) A photo of the aqueous solutions of N,S-CDs without (left) and with (right) 300 μM of Fe^{3+}. (b) Comparison of fluorescence intensities of N,S-CDs after adding different metal ions with the same concentration of 100 μM. (c) Fluorescence spectra of the N,S-CDs mixed with various concentrations of Fe^{3+}: 0, 25, 50, 75, 100, 125, 150, 175, 200, 300, 400 and 500 μM from top to bottom. (d) The emission intensity ratio F_0/F depends on the concentrations of the added Fe^{3+}, which is derived from the results in (c). F_0/F ratios are evaluated by the emission at 472 nm, and the excitation wavelength is set at 390 nm.

Fe^{3+} is an important metal ion in life because of its essential functions in oxygen transport, oxygen metabolism, electronic transfer and many catalytic processes.[10, 51] Fe^{3+} ions can be detected by CDs via luminescent measurement, but those published results suffered from the narrow ranges of detection concentrations,[51, 52] weak accuracy[33] or low selectivity.[10] Figure 7a exhibits the original N,S-CDs before and after quenching by Fe^{3+}. In comparison with many common metal ions (Figure 7b), only Fe^{3+} is able to quench the fluorescence of the N,S-CDs. Such specific fluorescence quenching effect may originate from the strong interactions between Fe^{3+} ions and the surface groups

of N,S-CDs which transfer the photoelectrons from CDs to Fe^{3+} ions.[10, 33] The fluorescence spectra of the N,S-CDs solution containing different concentrations of Fe^{3+} are measured under the excitation wavelength of 390 nm (Figure 7c). The ratios of F_0/F have a good linear correlation with the Fe^{3+} concentrations in the range of 25~500 μM (Figure 7d), much larger than those of recently reported values.[10, 33, 51, 52] Here F_0 and F are the fluorescent intensities of CDs at 472 nm in the absence and presence of Fe^{3+} ions, respectively. The quenching efficiency is fitted by the Stern-Volmer equation, $F_0/F = 1 + K_{SV}[Q]$, where K_{SV} is the Stern-Volmer quenching constant and [Q] is the Fe^{3+} concentration.[28] The K_{SV} value is calculated to be 2.85×10^3 L/mol with a correlation coefficient R^2 of 0.998. The detection limit is estimated to be 4 μM at a signal-to-noise ratio of 3.[53] The above results clearly prove that our CDs are very promising for Fe^{3+} detection in practical applications.

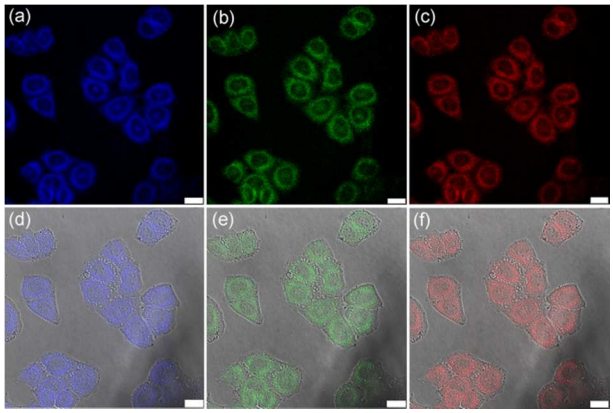

Fig. 8 Confocal fluorescence images of Hela cells after incubation with N,S-CDs (100 μg mL-1) for 2h. These images are obtained by (a) 405 nm excitation and the emission is recorded at 420~520 nm, (b) 458 nm excitation and the emission is recorded at 500~585 nm and (c) 514 nm excitation and the emission is recorded at 575~670 nm. The images (d-f) are the merged images of (a-c) with the corresponding bright field graphs. All scale bars represent 25 nm.

Before biological applications, the fluorescence stability of N,S-CDs under different pH values and ionic strength, long-time irradiation of UV or storage at ambient conditions, have been measured and illustrated in Figure S20. All results prove our N,S-CDs are very stable for practical applications. Cytotoxicity toward HeLa cells is performed through the conventional MTT assays (Figure S21).[54] The result shows after 48 h of incubation with N,S-CDs of 600 μg/mL, the cell viability is still over 80%. Thus we can safely use N,S-CDs of 100 μg/mL to incubate with HeLa cells for cell imaging. After 2 h incubation at 37 ℃ with 5 % CO_2, the cells are brightly illuminated and remain good morphologies under the confocal laser scanning microscope. These CDs mainly locate in the cytoplasm and they emit multicolor fluorescence under laser of different wavelengths (Figure 8), which further confirms these merits of our N,S-CDs.

4. Conclusions

Three kinds of CDs were synthesized respectively through the same route for comparison. These CDs had similar particle sizes and but different PL and QY. The N,S-CDs had the highest QY owing to the synergistic effect of nitrogen-sulfur co-doping. The optimal N,S-CDs showed excellent fluorescence stability, tunable emission color, high QY and low cytotoxicity, which ensured their successful applications in Fe^{3+} ions detection and multicolor cell imaging. Our present research confirms that both functional groups on the surface of CDs and aromatic structures in the cores of CDs, especially the C=N bonds, are very essential to improve photoluminescent properties of carbon dots.

Acknowledgements

This work was supported by National Major Basic Research Program of China (2013CB934101), the National Natural Science Foundation of China (21271045) and NCET-11-0115.

Notes and references

Department of Chemistry and Shanghai Key Laboratory of Molecular Catalysis and Innovative Materials, Fudan University, Shanghai 200433, P. R. China. E-mail: hmxiong@fudan.edu.cn

Electronic supplementary information (ESI) includes experimental details and comparable characterizations of three kinds of CDs.

1. S. N. Baker and G. A. Baker, *Angew. Chem. Int. Ed.*, 2010, **49**, 6726.
2.H. Li, Z. Kang, Y. Liu and S. T. Lee, *J. Mater. Chem.*, 2012, **22**, 24230.
3. R. Liu, D. Wu, S. Liu, K. Koynov, W. Knoll and Q. Li, *Angew.Chem. Int. Ed.*, 2009, **48**, 4598.
4. S. Liu, J. Tian, L. Wang, Y. Luo, J. Zhai and X. Sun, *J. Mater.Chem.*, 2011, **21**, 11726.
5. H. Li, X. He, Z. Kang, H. Huang, Y. Liu, J. Liu, S. Lian, C. H. Tsang, X. Yang and S. T. Lee, *Angew. Chem. Int. Ed.*, 2010, **49**, 4430.
6. X. Xu, R. Ray, Y. Gu, H. J. Ploehn, L. Gearheart, K. Raker and W. A. Scrivens, *J. Am. Chem. Soc.*, 2004, **126**, 12736.
7. G. Eda, Y. Y. Lin, C. Mattevi, H. Yamaguchi, H. A. Chen, I. S. Chen, C. W. Chen and M. Chhowalla, *Adv. Mater.*, 2010, **22**, 505.
8. S. Qu, X. Wang, Q. Lu, X. Liu and L. Wang, *Angew. Chem. Int. Ed.*, 2012, **51**, 12215.
9.Y. P. Sun, B. Zhou, Y. Lin, W. Wang, K. A. S. Fernando, P. Pathak, M. J. Meziani, B. A. ; Harruff, X. Wang and H. Wang, *J. Am. Chem. Soc.*, 2006, **128**, 7756.
10. S. Zhu, Q. Meng, L. Wang, J. Zhang, Y. Song, H. Jin, K. Zhang, H. Sun, H. Wang and B. Yang, *Angew. Chem. Int. Ed.*, 2013, **52**, 3953.
11. S. Liu, J. Tian, L. Wang, Y. Zhang, X. Qin, Y. Luo, A. M. Asiri, A. O. Al-Youbi and X. Sun, *Adv. Mater.*, 2012, **24**, 2037.
12. Z. L. Wu, M. X. Gao, T. T. Wang, X. Y. Wan, L. L. Zheng and C. Z. Huang, *Nanoscale*, 2014, **6**, 3868.
13. W. Kwon, S. Do, J. Lee, S. Hwang, J. K. Kim and S. W. Rhee, *Chem. Mater.*, 2013, **25**, 1893.
14. X. Gao, Y. Cui, R. M. Levenson, L. W. Chung and S. Nie, *Nat. Biotechnol.*, 2004, **22**, 969.
15. I. L. Medintz, H. T. Uyeda, E. R. Goldman and H. Mattoussi, *Nat. Mater.*, 2005, **4**, 435.

16. C. Zhu, J. Zhai and S. Dong, *Chem. Commun.*, 2012, **48**, 9367.
17. S. Sahu, B. Behera, T. K. Maiti and S. Mohapatra, *Chem. Commun.*, 2012, **48**, 8835.
18. D. Sun, R. Ban, P. H. Zhang, G. H. Wu, J. R. Zhang and J. J. Zhu, *Carbon*, 2013, **64**, 424.
19. Z. L. Wu, P. Zhang, M. X. Gao, C. F. Liu, W. Wang, F. Leng and C. Z. Huang, *J. Mater. Chem. B*, 2013, **1**, 2868.
20. Y. Q. Zhang, D. K. Ma, Y. Zhuang, X. Zhang, W. Chen, L. L. Hong, Q. X. Yan, K. Yu and S. M. Huang, *J. Mater. Chem.*, 2012, **22**, 16714.
21. Z. Qian, J. Ma, X. Shan, H. Feng, L. Shao and J. Chen, *Chem. Eur. J.*, 2014, **20**, 2254.
22. D. Qu, M. Zheng, L. Zhang, H. Zhao, Z. Xie, X. Jing, R. E. Haddad, H. Fan and Z. Sun, *Sci. Rep.,* 2014, **4,** 5294.
23. S. Chandra, P. Patra, S. H. Pathan, S. Roy, S. Mitra, A. Layek, R. Bhar, P. Pramanik and A. Goswami, *J. Mater. Chem. B*, 2013, **1**, 2375.
24. Y. Dong, H. Pang, H. B. Yang, C. Guo, J. Shao, Y. Chi, C. M. Li and T. Yu, *Angew. Chem. Int. Ed.*, 2013, **52**, 7800.
25. J. Deng, Q. Lu, N. Mi, H. Li, M. Liu, M. Xu, L. Tan, Q. Xie, Y. Zhang and S. Yao, *Chem. Eur. J.*, 2014, **20**, 4993.
26. D. Pan, J. Zhang, Z. Li and M. Wu, *Adv. Mater.*, 2010, **22**, 734.
27. H. Ding, P. Zhang, T. Y. Wang, J. L. Kong and H. M. Xiong, *Nanotechnology*, 2014, **25**, 205604.
28. M. Zheng, Z. Xie, D. Qu, D. Li, P. Du, X. Jing and Z. Sun, *ACS Appl. Mater. Interfaces*, 2013, **5**, 13242.
29. R. Ye, C. Xiang, J. Lin, Z. Peng, K. Huang, Z. Yan, N. P. Cook, E. L. Samuel, C. C. Hwang, G. Ruan, G. Ceriotti, A. R. Raji, A. A. Marti and J. M. Tour, *Nat. Commun.*, 2013, **4**, 2943.
30. M. X. Gao, C. F. Liu, Z. L. Wu, Q. L. Zeng, X. X. Yang, W. B. Wu, Y. F. Li and C. Z. Huang, *Chem. Commun.*, 2013, **49**, 8015.
31. H. Nie, M. Li, Q. Li, S. Liang, Y. Tan, L. Sheng, W. Shi and S. X.-A. Zhang, *Chem. Mater.*, 2014, **26**, 3104.
32. D. M. Wang, M. X. Gao, P. F. Gao, H. Yang and C. Z. Huang, *J. Phys. Chem. C*, 2013, **117**, 19219.
33. W. Li, Z. Zhang, B. Kong, S. Feng, J. Wang, L. Wang, J. Yang, F. Zhang, P. Wu and D. Zhao, *Angew.Chem. Int. Ed.*, 2013, **52**, 8151.
34. J. Zhou, Y. Yang and C. Y. Zhang, *Chem. Commun.*, 2013, **49**, 8605.
35. M. J. Bojdys, J. O. Muller, M. Antonietti and A. Thomas, *Chem. Eur. J.*, 2008, **14**, 8177.
36. Yang Z, Yao Z, Li G, Fang G, Nie H, Liu Z, X. M. Zhou, X. A. Chen and S. M. Huang, *ACS Nano*, 2012, **6**, 205.
37. Y. Deng, D. Zhao, X. Chen, F. Wang, H. Song and D. Shen, *Chem. Commun.*, 2013, **49**, 5751.
38. B. X. Zhang, H. Gao and X. L. Li, *New. J. Chem.*, 2014, **38**, 4615.
39. Y. Wang and A. Hu, *J. Mater. Chem. C*, 2014, **2**, 6921.
40. M. J. Krysmann, A. Kelarakis, P. Dallas and E. P. Giannelis, *J. Am. Chem. Soc.*, 2012, **134**, 747.
41. Z. Q. Xu, L. Y. Yang, X. Y. Fan, J. C. Jin, J. Mei, W. Peng, F. L. Jiang, Q. Xiao and Y. Liu, *Carbon*, 2014, **66**, 351.
42. H. Tao, K. Yang, Z. Ma, J. Wan, Y. Zhang, Z. Kang and Z. Liu, *Small*, 2011, **8**, 281.
43. Y. Wang, S. Kalytchuk, Y. Zhang, H. Shi, S. V. Kershaw and A. L. Rogach, *J. Phys. Chem. Lett.*, 2014, **5**, 1412.
44. S. Zhu, J. Zhang, S. Tang, C. Qiao, L. Wang, H. Wang, X. Liu, B. Li, Y. Li, W. Yu, X. Wang, H. Sun and B. Yang, *Adv. Funct. Mater.*, 2012, **22**, 4732.
45. H. Zheng, Q. Wang, Y. Long, H. Zhang, X. Huang and R. Zhu, *Chem. Commun.*, 2011, **47**, 10650.
46. X. Wen, P. Yu, Y. R. Toh, X. Ma and J. Tang, *Chem. Commun.*, 2014, **50**, 4703.
47. S. L. Hu, K. Y. Niu, J. Sun, J. Yang, N. Q. Zhao and X. W. Du, *J. Mater. Chem.*, 2009, **19**, 484.
48. J. Liang, Y. Jiao, M. Jaroniec and S. Z. Qiao, *Angew. Chem. Int. Ed.*, 2012, **51**, 11496.
49. S. A. Wohlgemuth, R. J. White, M. G. Willinger, M. M. Titirici and M. Antonietti, *Green Chem.*, 2012, **14**, 1515.
50. D. Qu, M. Zheng, P. Du, Y. Zhou, L. Zhang, D. Li, H. Tan, Z. Zhao, Z. Xie and Z. Sun, *Nanoscale*, 2013, **5**, 12272.
51. K. Qu, J. Wang, J. Ren and X. Qu, *Chem. Eur. J.*, 2013, **19**, 7243.
52. T. Lai, E. Zheng, L. Chen, X. Wang, L. Kong, C. You, Y. Ruan and X. Weng, *Nanoscale*, 2013, **5**, 8015.
53. C. Hu, C. Yu, M. Li, X. Wang, J. Yang, Z. Zhao, A. Eychmuller, Y. P. Sun and J. Qiu, *Small*, 2014, DOI:10.1002/smll.201401328.
54. H. Ding, L. W. Cheng, Y. Y. Ma, J. L. Kong and H. M. Xiong, *New. J. Chem.*, 2013, **37**, 2515.